Journal of Pharmaceutical and Biomedical Analysis 251 (2024) 116451

Contents lists available at ScienceDirect

Journal of Pharmaceutical and Biomedical Analysis

journal homepage: www.journals.elsevier.com/journal-of-pharmaceutical-and-biomedical-analysis

Metabolic signatures of metabolites of the purine degradation pathway in human plasma using HILIC UHPLC–HRMS

Rui Liu [a,1], Qingke Wu [a,1], Chuanlong Wu [a], Yingnan Qu [a], Yanming Fang [a], Jiyangzong De [a], Ronghua Fan [a,b,*], Wenjing Song [a,**]

[a] School of Public Health, Shenyang Medical College, Shenyang 110034, China
[b] Key Lab of Environmental Pollution and Microecology of Liaoning Province, Shenyang 110034, China

ARTICLE INFO

Keywords:
Purine intermediates
HILIC
ROC analysis
Purine degradation pathway
Risk factor

ABSTRACT

The metabolic disorders in the purine degradation pathway have proven to be closely associated with several human diseases. However, the etiology is not yet fully understood. Profile assay of purine intermediates and uric acid involved in the metabolic pathway can provide additional insight into the nature and severity of related diseases. Purine metabolites are endogenous chemicals with high hydrophilicity, polarity, and similar structures, thus there is a great need for a specific method to quantify them directly in biological fluids with a short running time. Herein, eight purine degradation pathway metabolites, including xanthine, hypoxanthine, guanine, xanthosine, inosine, guanosine, adenosine and uric acid, in human plasma were quantitatively measured using hydrophilic interaction chromatography-tandem high-resolution mass spectrometry (HILIC-HRMS) in a short running time of 10 min. The method was systematically validated for specificity, linearity of the calibration curve, the limit of detection, the limit of quantification, the lower limit of quantification, precision, accuracy, extraction recovery, matrix effect, and stability. The results showed that the method was linear ($R^2 > 0.99$), accurate (the intra- and inter-day recoveries of all analytes ranged from 90.0 % to 110.0 %), and precise (the intra- and inter-day precisions were less than 6.7 % and 8.9 %, respectively) with the lower limits of quantification ranging from 3 to 10,000 ng/mL. The extraction recoveries and matrix effects were repeatable and stable. All the analytes were stable in the autosampler and could be subject to three freeze-thaw cycles. The developed method was ultimately applied to 100 plasma specimens from healthy individuals. The results showed that the concentrations of different purine metabolites varied dramatically in plasma specimens. Diet and body mass index (BMI) were the most significant factors determining purine levels, followed by drinking and sex. Age, smoking and bedtime showed a very weak correlation with purine metabolism. The findings of the present work reveal the characteristics of purine metabolism in human plasma under non-pathological conditions. The results also highlight the factors that can cause changes in purine metabolism, which are useful in developing effective treatment strategies for metabolic disorders of purines, particularly for those caused by lifestyle factors.

1. Introduction

Purines are groups of nitrogenous bases that not only serve as the fundamental building blocks of deoxyribonucleic acid (DNA) and ribonucleic acid (RNA) but also participate in many other important physiological functions [1]. Some purines, such as adenosine triphosphate (ATP) and guanosine triphosphate (GTP), are directly involved in cellular energy supply, while others act as cofactors, for example, nicotinamide adenine dinucleotide (NAD+) plays key roles in glucose breakdown and energy production [2]. In addition, purines also function as intracellular and extracellular signaling molecules that can bind to cell surface receptors, triggering a chain of events that ultimately affect cellular behavior [3].

Most purines can be synthesized endogenously through a salvage pathway that reuses purines from damaged or dying cells [4]. A small portion of them also come from the digestion of food and the

* Corresponding author at: School of Public Health, Shenyang Medical College, Shenyang 110034, China.
** Corresponding author.
E-mail addresses: fanronghua@symc.edu.cn (R. Fan), wjsong@symc.edu.cn (W. Song).
[1] Rui Liu and Qingke Wu contributed equally

https://doi.org/10.1016/j.jpba.2024.116451
Received 9 May 2024; Received in revised form 16 July 2024; Accepted 23 August 2024
Available online 26 August 2024

degradation of RNA and DNA, a de novo synthesis that newly creates purines [4]. The breakdown of purines follows a catabolic pathway involving several steps [5], as illustrated in Fig. 1. Ultimately, uric acid is produced as the final compound, which is then excreted from the body through urine. It is worth noting that uric acid accounts for approximately 60 % of a human's total antioxidant activity and is considered neuroprotective [2]. However, high levels of serum urate can lead to a variety of disorders.

It has been widely accepted for a long time that hyperuricemia, caused by the overproduction of uric acid [6], increases the risks of gout [6], gouty arthritis [7] obesity [8], adiposity-related non-alcoholic fatty liver disease (NAFLD) [9,10], type 2 diabetes [11], cardiovascular disease (CVD) [12,13], neurodegenerative disease [14,15], cancer [16], and chronic kidney disease (CKD) [17,18]. In these diseases, uric acid has a strong potential as a therapeutic target. To better understand the relationship between urine acid levels and purine metabolic malfunction in human plasma, it is necessary to monitor the concentrations of metabolites involved in the purine pathway.

Numerous chromatographic methods have been reported for the quantification of most of the metabolites of the purine catabolic pathway in human tissues and biological fluids. Reversed-phase (RP) HPLC [19–21] and capillary electrochromatography (CEC) [22,23] with ultraviolet (UV) detection are used to quantify uric acid, xanthine, hypoxanthine, allantoin, guanine, adenine, adenosine, cytidine, or N6-methyladenosine in human plasma/serum and urine. Although these methods are low-cost, the number of target analytes and sensitivity are very limited. With the application of mass spectrometry (MS) as a detector after chromatographic separation, more purines can be detected with higher sensitivity [24,25]. Unfortunately, purine metabolites are endogenous compounds with high hydrophilicity, polarity, and similar chemical structures, it is a challenging task to quantify simultaneously in biological fluids. They suffer from poor retention and resolution on the RP column, leading to interference by the co-eluted matrix. To overcome this issue, ion-pairing (IP) reagents, such as tetrabutylammonium hydroxide (TBAH) [26], diethylamine (DEA) [27], hexafluoro-2-propanol (HFIP) [27], and tetrabutylammonium hydrogen sulfate (TBAHS) [28], have been used to improve the retention behaviors and peak symmetries of purine metabolites in RP LC system. Despite this, the use of IP reagents can cause ion source contamination and reduce instrumental sensitivity due to its low volatility and potentiality of significant ion suppression [29].

Hydrophilic interaction chromatography (HILIC), a kind of normal-phase liquid chromatography (NPLC), is considered the most suitable for separating polar molecules in a wide variety of scientific fields, including pharmaceutical chemistry, agricultural and food chemistry, medicinal chemistry, proteomics, metabolomics, and glycomics. This method is particularly useful for separating biomarkers, amino acids, purines, nucleosides, nucleotides, carbohydrates, peptides, and proteins [30]. While some studies have delved into the use of the HILIC tandem triple quadrupole MS (HILIC–QqQ–MS) for the simultaneous determination of metabolites in the purine pathway [29–32], there are currently no reports on the detection of the metabolites in human plasma using HILIC coupled with high-resolution MS (HRMS). HRMS is considered the optimal tool for addressing the complexities of mass measurement, with the ability to measure mass in many decimal places. In contrast, the conventional MS is supposed to measure nominal mass. HRMS has a mass accuracy of less than 5 parts per million (ppm), and its mass resolution allows for peak discrimination and increased separation. Many studies have demonstrated that the HRMS instruments showed similar quantitative performance to QqQ–MS. Importantly, HRMS can be as

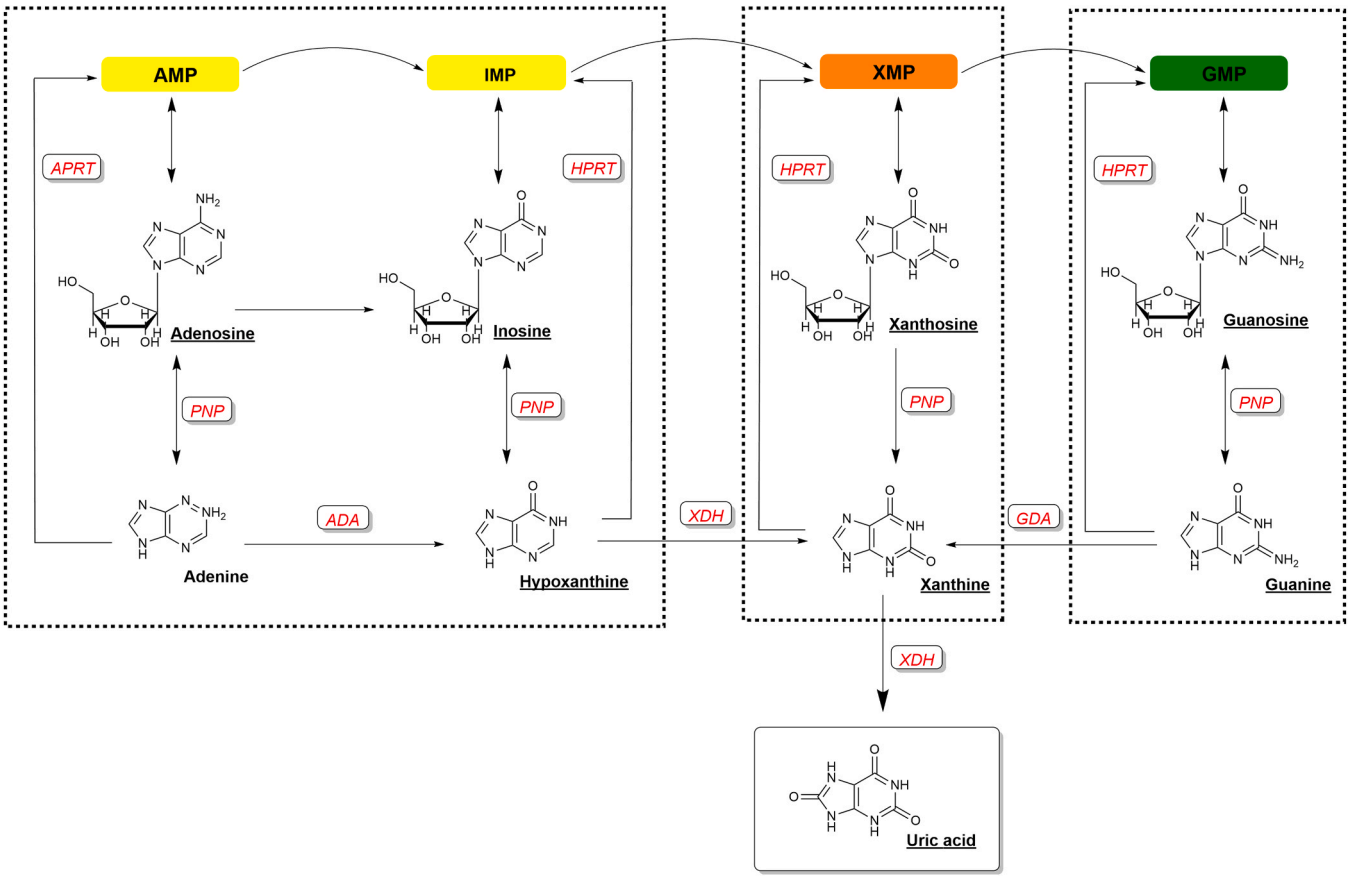

Fig. 1. Simplified scheme of purine degradation pathway. The eight underlined metabolites were quantified in the present study. AMP, adenosine monophosphate; IMP, inosine monophosphate; XMP, xanthosine monophosphate; GMP, guanosine monophosphate; APRT, adenine phosphoribosyl transferase; HPRT, hypoxanthine-guanine phosphoribosyl transferase; PNP, purine nucleoside phosphorylase; ADA, adenine deaminase; XDH, xanthine dehydrogenase; GDA, guanine deaminase.

sensitive and selective in HR-full scan as QqQ–MS in selected reaction monitoring (SRM) acquisition [33]. HILIC–HRMS can perform excellent quantitative determinations of polar analytes in biological samples with increased confidence and accuracy.

In the present study, a simple and efficient HILIC-HRMS method was developed and validated to simultaneously quantify eight metabolites of the purine degradation pathway in healthy human plasma. Included were xanthine, hypoxanthine, guanine, xanthosine, inosine, guanosine, adenosine, and uric acid. In comparison to QqQ-MS, this method utilized first-stage MS for quantification without the need to optimize precursor ion and product ion parameters. Instead, it relied only on the precise molecular mass of the target analytes for accurate quantification, thus offering faster analysis. Moreover, since purine metabolism involves a multifactorial interplay of general state, physical characteristics, and lifestyle, concentration changes of the eight metabolites with respect to these factors were also evaluated. The results of this study could provide further information on metabolic alterations and pathophysiologic mechanisms involved.

2. Material and methods

2.1. Chemicals and reagents

Reference standards with a purity of ⩾ 98 % of xanthine, hypoxanthine, guanine, xanthosine, inosine, guanosine, adenosine and uric acid were purchased from Sigma-Aldrich (St. Louis, Missouri, US). Fig. 1 depicts the chemical structures of these reference compounds. LC-MS grade acetonitrile (ACN), methanol (MeOH), ammonium formate, and formic acid were purchased from Merck (Darmstadt, Germany). Anhydrous sodium hydroxide (NaOH, > 98 %) was obtained from Sigma-Aldrich (St. Louis, Missouri, US). Synthetic plasma was purchased from IPHASE (Suzhou, China) and used as the blank matrix. This synthetic plasma (pH 7.4) contains calcium chloride, sodium chloride, sodium sulfate, sodium bicarbonate, dipotassium hydrogen phosphate, sodium sulfate, and other components. The other reagents were all the analytical grades. Ultrapure water (18.2 MΩ) used for the preparation of the mobile phases and the standards were purified by a Milli-Q purification system (Milford, MA, USA).

2.2. Preparation of standard solutions and quality control samples

The individual standards were weighed separately and dissolved in 0.1 mol/L NaOH to achieve a concentration of 1 mg/mL, except for guanine (0.1 mg/mL) and uric acid (2 mg/mL). All the stock solutions were kept at −80℃. Before use, working solutions were prepared freshly by mixing different volumes of the individual stock solutions and diluting them with 80 % ACN (*v/v*). Calibrants and Quality Control samples (QCs) at low (LQC), medium (MQC), and high (HQC) concentrations were prepared by spiking synthetic plasma with working solutions and then pretreating as described in Section 2.3. The calibrants covered a range of 0.05–10 μg/mL for xanthine; 0.1–10 μg/mL for hypoxanthine; 0.005–2 μg/mL for guanine; 0.15–15 μg/mL for xanthosine; 0.01–1 μg/mL for inosine; 0.003–0.1 μg/mL for guanosine; 0.03–3 μg/mL for adenosine; 10–100 μg/mL for uric acid. The detailed concentrations of the calibrants are provided in Table S1 of the Supporting Information. Moreover, the LQC concentration was three times the lower limit of quantitation (LLOQ). The MQC and HQC concentrations were around 30–50 % of the calibration curve range and at least 75 % of the upper limit of quantitation (ULOQ). The ULOQ represented the highest concentration on the calibration curve. The concentrations for the QCs were as follows: xanthine (0.15, 2.4 and 8 μg/mL), hypoxanthine (0.3, 5 and 8 μg/mL), guanine (0.015, 0.32 and 1.6 μg/mL), xanthosine (0.045, 5 and 12 μg/mL), inosine (0.03, 0.5 and 0.8 μg/mL), guanosine (0.009, 0.04 and 0.08 μg/mL), adenosine (0.09, 1.2 and 2.4 μg/mL), and uric acid (30, 45 and 90 μg/mL). All solutions were stored at 4℃ prior to use.

2.3. Sample collection and preparation

Human blood samples were collected from 100 healthy volunteers, 50 males and 50 females with a mean age of 31.7 ± 10.8 years old. All participants underwent their physical checkups. They did not take any drugs or nutrition during the research. Shenyang Medical College approved the protocol of the study (Grant number: SYMC-20201230–08).

The blood samples were collected using EDTA-K2 test tubes and then removed to new Eppendorf tubes after centrifugation at 3500 ×g for 5 min at 4℃. All samples were stored at −80℃ freezer until analysis. For plasma sample preparation, 100 μL plasma was added to 400 μL ACN for protein precipitation. After vortex for 1 min and centrifugation at 15,000 ×g under 4℃ for 10 min, 300 μL the supernatant was evaporated under nitrogen and completely freeze-dried. The dried residue was then redissolved in 75 μL of 80 % ACN and kept at 4℃ for subsequent UHPLC-HRMS analysis.

Data on general states and lifestyle habits were collected using a self-administered questionnaire (Fig. S1 in Supporting Information). General states including age and sex. Lifestyle factors such as smoking, drinking, diet, and bedtime were considered in the questionnaire. Table S2 in Supporting Information displays the baseline characteristics of the participants. The age ranges were split into three groups: 18–25, 26–35, and 36–45 years. Normal-purine diet (NPD) participants were prescribed to consume a regular purine diet, while the rich-purine diet (RPD) group was prescribed to consume meats, poultry, seafood, organ meats, alcohol (including beer), and fructose-rich foods. Participants were also classified as smokers or nonsmokers based on their smoking status. Moreover, the participants were asked, "How frequently did you drink during a week?" One of the following three options could be selected: never, 1–2 days/week (occasionally), or 3–7 days/week (often). Bedtime was categorized as normal (before 21:00), late (21:00–24:00), or night owl (after 24:00).

A digital scale with a precision of 0.1 cm for height measurements and 0.01 kg for weight measurements was utilized to determine body mass index (BMI). BMI was calculated as weight divided by height squared. According to the guidelines set by the National Heart, Lung, and Blood Institute (NHLBI), individuals with a BMI less than 18.5 kg/m^2 were classified as underweight [34]. Normal weight, overweight, low obesity and medium obesity were defined as BMI falling within the ranges of 18.5–25, 25–30, 30–35 and 35–40 kg/m^2, respectively. Those with a BMI of 40 kg/m^2 or greater were considered extremely obesity.

2.4. HILIC-HRMS conditions

The HILIC-UHPLC-HRMS analysis was performed using an UltiMate 3000 series UHPLC system coupled to a Q-Exactive Orbitrap tandem MS via an electrospray ionization (ESI) interface (ThermoFisher Scientific, Bremen, Germany). The HILIC Amide Column (3.0 mm × 150 mm, 1.7 μm particle size) was supplied by Qiao's research group, and its preparation method is described in reference [35]. The column temperature was set at 35°C. Elution was performed at 0.4 mL/min using a binary mobile phase system consisting of A: 5 mmol/L ammonium formate (adjust pH to 3 with formic acid) in water and B: 5 mmol/L ammonium formate (adjust pH to 3 with formic acid) in ACN. Adjustment to pH 3 was performed in the aqueous phase before mixing with the organic solvent. The linear gradient conditions were as follows: 0–3 min, 83 % B; 3–10 min, 83–73 % B. The injection volume was 5.0 μL.

The HRMS spectrometer was operated in positive ionization mode. The MS conditions were spray voltage, 4.0 kV; capillary temperature, 320°C; auxiliary gas heating temperature, 320°C; sheath gas pressure, 40 arb; auxiliary gas pressure, 10 arb; sweep gas pressure, 5 arb; S-lens RF, 55. Ions were monitored by full scan mode in the range of 50–500 *m/z*. The instrument was calibrated every 24 h. Data were processed using XcaliburTM software (Version 2.1.1, ThermoFisher Scientific).

2.5. Method validation

Method performance was validated in terms of specificity, linearity, the limit of detection (LOD), the limit of quantification (LOQ), LLOQ, precision, accuracy, extraction recovery, matrix effect, and stability.

2.5.1. Specificity

The specificity was checked by comparing the retention time (RT) and HRMS spectra of each analyte in plasma samples with their corresponding standards.

2.5.2. Linearity and sensitivity

Linearity was determined by constructing calibration curves. Calibration curves were established by plotting the peak area of each analyte against the corresponding concentration of mixed working standard solutions using a weighted least squares linear regression model ($1/\chi^2$). Each calibration curve was generated by seven concentrations, and three replicates were performed for each concentration level. The concentrations of mixed working standard solutions are listed in Table S1. The linearity was characterized by the determination coefficient (R^2). Moreover, LOD and LOQ were estimated by diluting mix standards solutions which were able to generate signal-to-noise (S/N) ratios of 3 and 10, respectively. LLOQ was defined as the lowest concentration on the calibration curve.

2.5.3. Precision, accuracy, and recovery

Intra-day precision was assessed by analyzing six replicates of the QCs at four spiking levels (LLOQ, LQC, MQC and HQC) within one day ($n = 6$). For inter-day precision, six replicates of the QCs were analyzed thrice per day over three consecutive days ($n = 3 \times 3$). Accuracy was calculated using the same set of QCs by comparing the measured concentrations with their nominal concentrations. The concentration for each analyte was calculated using the calibration prepared on the same day. The precision was expressed as the relative standard deviation (RSD, %). The acceptable criteria of precision and accuracy should be within ±20 % and 80–120 % respectively at the LLOQ. For the other QC levels, precision should be less than 15 % and accuracy should be in the range of 85–115 %.

2.5.4. Extraction recovery and matrix effect

Both extraction recovery and matrix effect were measured by using LQC, MQC and HQC samples. Extraction recovery was estimated by determining six replicates of QCs before and after extraction ($n = 6$). Synthetic plasma was used as the blank biological matrix. The recovery (%) was the measured concentration divided by the nominal concentration that was spiked into extracted synthetic plasma. For the matrix effect, the analyte peak area in extracted synthetic plasma was divided by the peak area in 80 % ACN. Both the extraction recovery and matrix effect should be consistent with 85–115 %, and the LQC should be consistent with 80–120 %.

2.5.5. Stability

The stability was performed by analyzing six replicates at LQC and HQC levels under two conditions: the samples were kept at 4℃ in an autosampler for 24 h and subjected to three freeze-thaw cycles. RE% was used to evaluate the stability. The acceptable RE% should be within ±15 % and the low-concentration QC samples should not exceed 20 %.

2.6. Statistical analysis

The experimental values were expressed as the mean ± standard deviation (SD). Differences between two groups with normal distribution were analyzed by one-way ANOVA followed by the Holm-Sidak method for multiple comparisons using SPSS 25.0 software (Chicago, IL, USA). Data not normally distributed were analyzed by Kruskal-Wallis ANOVA on Ranks followed by Dunnet's test. $p < 0.05$ was considered a significant difference. The receiver operating characteristic (ROC) curve of uric acid was performed by SPSS 25.0 software (Chicago, IL, USA).

3. Results and discussion

3.1. Method development and optimization

A series of tests was performed to achieve better chromatographic behavior for all eight metabolites. Initially, we investigated the separation using an Ultimate XB-C8 column (2.1 mm × 150 mm, 2.7 μm, Welch, Shanghai, China) and a Boltimate C18 column (2.1 mm × 150 mm, 2.7 μm, Welch, Shanghai, China); however, the results were not satisfactory. As indicated in Fig. S2A and B (Supporting Information), all eight analytes were eluted within the first 2 min. Consequently, for this study, an HILIC column was chosen. We tested two types of HILIC columns: the commercialized Ultimate HILIC column (3.0 mm × 150 mm, 3 μm, Welch, Shanghai, China) and the HILIC Amide column (3.0 mm × 150 mm, 1.7 μm) supplied by Qiao's research group. The results are displayed in Fig. S2C and D in Supporting Information. The latter HILIC column demonstrated symmetrical peak shape and satisfactory separation, apart from xanthosine and inosine, as well as guanosine and uric acid, which could not achieve baseline separation from each other. Fortunately, HRMS analysis facilitated the distinction of xanthosine and inosine, as well as guanosine and uric acid, due to the difference in their molecular weights.

Next, we optimized the mobile phase system. As shown in Fig. S3A (Supporting Information), all the analytes were eluted within approximately 5 min using a MeOH-water solvent system. The ACN-water solvent system exhibited weak elution capacity, resulting in more chromatographic peaks in the chromatogram (Fig. S3B in Supporting Information). We then focused on optimizing the mobile phase additive. The addition of ammonium formate significantly enhanced the separation and signal intensity of the analytes (Fig. S3C in Supporting Information). However, we found that the concentration of ammonium formate and pH value had minimal impact on the separation. Taking into account reproducibility and common practices in the literature, we chose a concentration of 5 mmol/L for ammonium formate and adjusted the pH to 3 with formic acid.

Finally, other eluting parameters, such as elution gradient and flow rate were optimized, and the best chromatographic separation was achieved as outlined in Section 2.4. The representative extracted ion chromatograms (EICs) are displayed in Fig. 2. All eight analytes were eluted successfully within a short timeframe of 3–8 min. This rapid elution process not only enhanced experimental efficiency but also minimized solvent usage and analytical expenses. The analytes were efficiently separated from each other, demonstrating good selectivity to distinguish closely related analytes and avoid peak overlap.

3.2. Method validation

The specificity of the developed method was assessed by qualitatively comparing the EICs of the eight analytes from both plasma and mixed standards in 80 % ACN (v/v). As seen in Fig. 2, the RTs of each analyte in human plasma (Fig. 2B) were well consistent with those in the standard mixture (Fig. 2A). No significant endogenous interferences were detected around the RTs of analytes in the samples of human plasma (Fig. 2B). Further, upon careful examination of the EICs, we did not find additional ions sharing the same RTs and base peak m/z. These findings were indicative of good peak purity and provided confidence in the specificity of the method for the detection and quantification of the target analytes.

The calibration curve, LODs, LOQs and more detailed information regarding the eight metabolites are listed in Table 1. Good linearities over two orders of magnitude were achieved for all analytes with R^2 in the range of 0.9931–0.9993. The LOD values ranged from 1 ng/mL to 9 ng/mL, whereas LOQ values were between 2 ng/mL and 30 ng/mL.

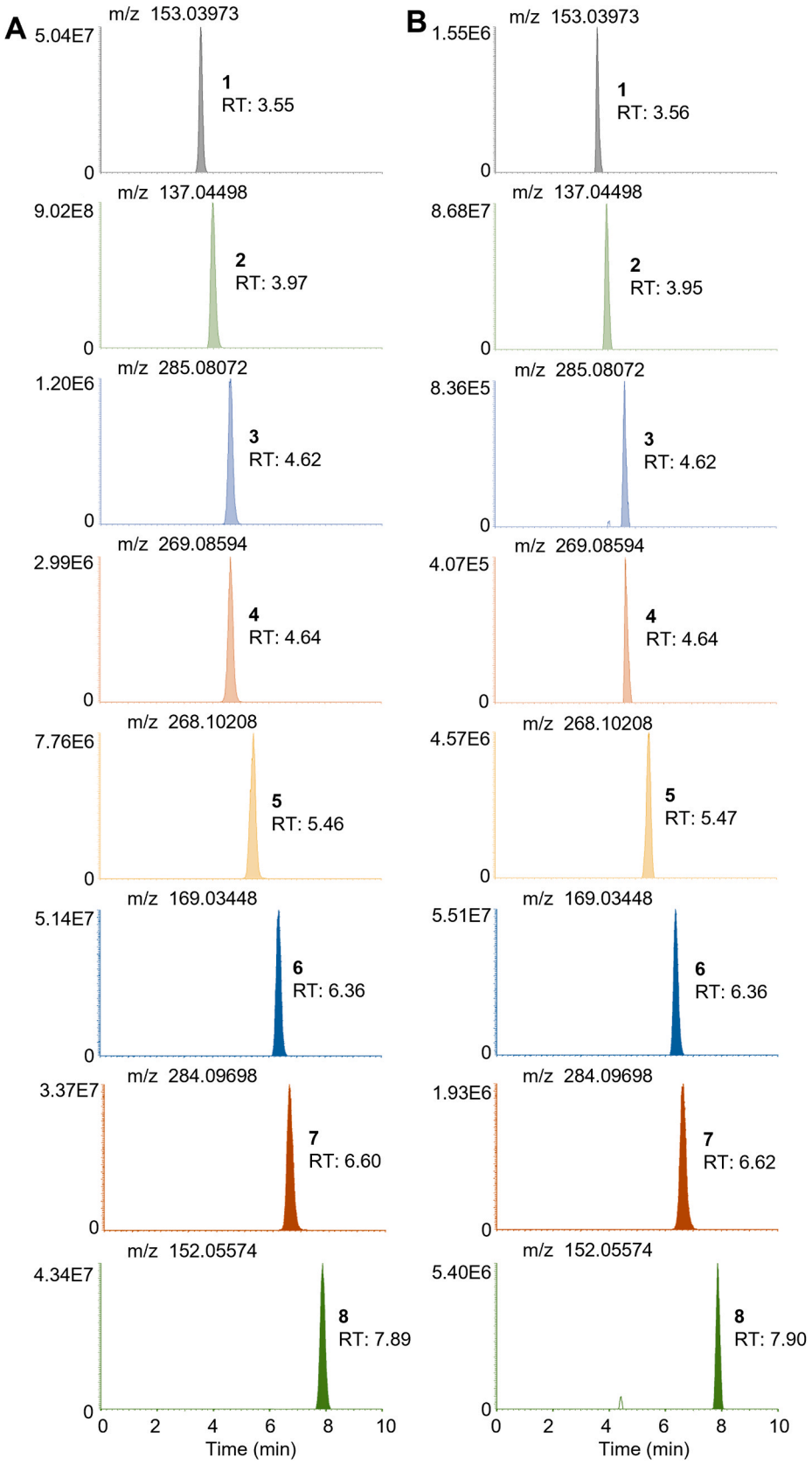

Fig. 2. Extracted ion chromatograms (EICs) of eight targeted metabolites. (A) Representative EICs in 80 % ACN (*v/v*). (B) Representative EICs in human plasma samples. The metabolites are as follows, xanthine (1), hypoxanthine (2), xanthosine (3), inosine (4), adenosine (5), uric acid (6), guanosine (7), guanine (8).

Table 1
Summary of calibration equation, determination coefficient (R^2), linear range, the limit of detection (LOD), the limit of quantification (LOQ), and the lower limit of quantitation (LLOQ) of the eight metabolites obtained using the HILIC–HRMS method.

No.	Metabolites	Calibration equation[a]	R^2	Linear range (ng/mL)	LOD (ng/mL)	LOQ (ng/mL)	LLOQ (ng/mL)
1	Xanthine	$y = 4.01\times10^3x + 5.78\times10^3$	0.9945	50–10,000	9	30	50
2	Hypoxanthine	$y = 1.60\times10^5x + 3.77\times10^5$	0.9953	100–10,000	4	10	100
3	Guanine	$y = 1.60\times10^5x+3.12\times10^4$	0.9931	5–2000	1	2	5
4	Xanthosine	$y = 9.59\times10^3x + 8.41\times10^3$	0.9968	150–15,000	8	30	150
5	Inosine	$y = 8.38\times10^3x + 4.39\times10^3$	0.9967	10–1000	3	10	10
6	Guanosine	$y = 1.63\times10^4x + 2.92\times10^3$	0.9971	3–100	1	3	3
7	Adenosine	$y = 4.80\times10^4x + 4.85\times10^4$	0.9993	30–3000	3	10	30
8	Uric acid	$y = 1.70\times10^3x + 2.43\times10^4$	0.9982	10,000–100,000	6	20	10,000

[a] For external calibration, y = peak area of analyte; x = concentration of analyte.

The results indicated that the method was reliable and reproducible for the determination of metabolites in the purine pathway in human plasma.

The RSDs of intra-day and inter-day precision results for the detection of the LLOQ, LQC, MQC and HQC samples were lower than 6.7 % and 8.9 %, respectively, as presented in Table 2. At the three concentration levels, the intra-day and inter-day accuracy ranged between 90.0 % and 110.0 % (Table 2). Both precision and accuracy were within acceptable ranges. The extraction recoveries of these metabolites were measured by determining synthetic plasma with the mixed standards at low, medium and high concentrations, and protein precipitation resulted in an overall recovery of 91.1–108.7 % (data shown in Table 3). Meanwhile, the matrix effect results are also presented in Table 3. The values ranged from 90.9 % to 106.9 %, which proved that the plasma samples were extracted efficiently by protein precipitation with a minor matrix effect. The autosampler and freeze-thaw stability of the eight metabolites were determined, as shown in Table 4. QC samples of two concentration levels (LQC and HQC) were stable in the autosampler and samples could undergo three cycles of freezing at −80°C and thawing at room temperature without affecting the stability of the eight analytes. In summary, the proposed HILIC-HRMS method was accurate, sensitive, and repeatable enough for the qualification of the eight target analytes in human plasma.

3.3. Application to plasma sample assay

The newly developed HILIC–HRMS method was applied to analyze a total of 100 plasma samples collected from a cohort of healthy individuals. One of the key challenges encountered in this study involved selecting an appropriate and inexpensive internal standard with chemical characteristics similar to the seven purines and uric acid. As a result, the choice was made to employ an external standard calibration method, which underwent rigorous validation procedures to guarantee the production of precise and reliable outcomes. Xanthine, hypoxanthine, guanine, xanthosine, adenosine and uric acid were successfully detected and quantified, while in some plasma samples, the concentrations of

Table 2
Accuracy and precision.

Metabolites	Level	Nominal concentration (μg/mL)	Intra-day (n = 6)			Inter-day (n = 9)		
			Concentration measured ± SD (μg/mL)	Accuracy[a] (%)	Precision (RSD, %)	Concentration measured ± SD (μg/mL)	Accuracy (%)	Precision (RSD, %)
Xanthine	LLOQ	0.05	0.047 ± 0.003	94.0	4.0	0.045 ± 0.003	90.0	6.0
	LQC	0.15	0.164 ± 0.007	109.3	4.6	0.139 ± 0.008	92.7	5.3
	MQC	2.4	2.527 ± 0.079	105.3	3.3	2.551 ± 0.072	106.3	3.0
	HQC	8	7.673 ± 0.324	95.9	4.1	8.584 ± 0.280	107.3	3.5
Hypoxanthine	LLOQ	0.1	0.096 ± 0.005	96.0	5.0	0.107 ± 0.006	107.0	6.0
	LQC	0.3	0.328 ± 0.019	109.3	6.3	0.296 ± 0.014	98.7	4.7
	MQC	5	4.975 ± 0.190	99.5	3.8	5.410 ± 0.145	108.2	2.9
	HQC	8	7.656 ± 0.345	95.7	4.3	8.616 ± 0.227	107.7	2.8
Guanine	LLOQ	0.005	0.0054 ± 0.0002	108.0	4.0	0.0046 ± 0.0002	92.0	4.0
	LQC	0.015	0.016 ± 0.001	106.7	6.7	0.014 ± 0.001	93.3	6.7
	MQC	0.32	0.323 ± 0.003	100.9	0.9	0.330 ± 0.008	103.1	2.5
	HQC	1.6	1.541 ± 0.057	96.3	3.6	1.534 ± 0.061	95.9	3.8
Xanthosine	LLOQ	0.15	0.164 ± 0.005	109.3	3.3	0.140 ± 0.007	93.3	4.7
	LQC	0.045	0.042 ± 0.002	93.3	4.4	0.049 ± 0.004	108.9	8.9
	MQC	5	5.205 ± 0.105	104.1	2.1	4.630 ± 0.205	92.6	4.1
	HQC	12	11.23 ± 0.48	93.6	4.0	11.62 ± 0.29	96.8	2.4
Inosine	LLOQ	0.01	0.0095 ± 0.0004	100.0	4.0	0.0110 ± 0.0006	110.0	6.0
	LQC	0.03	0.028 ± 0.001	93.3	3.3	0.032 ± 0.001	106.7	3.3
	MQC	0.5	0.474 ± 0.024	94.8	4.8	0.498 ± 0.019	99.6	3.8
	HQC	0.8	0.876 ± 0.034	109.5	4.3	0.749 ± 0.043	93.6	5.4
Guanosine	LLOQ	0.003	0.0028 ± 0.0002	93.3	6.7	0.0029 ± 0.0002	96.7	6.7
	LQC	0.009	0.0094 ± 0.0005	104.4	5.6	0.0093 ± 0.0004	103.3	4.4
	MQC	0.04	0.043 ± 0.001	107.5	2.5	0.043 ± 0.001	107.5	2.5
	HQC	0.08	0.083 ± 0.004	103.8	5.0	0.085 ± 0.003	106.3	3.8
Adenosine	LLOQ	0.03	0.029 ± 0.001	96.7	3.3	0.032 ± 0.001	106.7	3.3
	LQC	0.09	0.083 ± 0.003	92.2	3.3	0.097 ± 0.004	107.8	4.4
	MQC	1.2	1.304 ± 0.047	108.7	3.9	1.261 ± 0.034	105.1	2.8
	HQC	2.4	2.323 ± 0.076	96.8	3.2	2.270 ± 0.088	94.6	3.7
Uric acid	LLOQ	10	10.25 ± 0.43	102.5	4.3	10.36 ± 0.41	103.6	4.1
	LQC	30	28.38 ± 1.67	94.6	5.6	31.92 ± 1.08	106.4	3.6
	MQC	45	45.76 ± 0.91	101.7	2.0	43.79 ± 0.68	97.3	1.5
	HQC	90	88.47 ± 1.62	98.3	1.8	87.03 ± 1.17	96.7	1.3

[a] Accuracy = (Concentration measured / Nominal concentration) × 100 %.

Table 3
Extraction recovery and matrix effect ($n = 6$).

Metabolites	Level	Nominal concentration (μg/mL)	Measured concentration ± SD (μg/mL)	Recovery[a] mean ± SD (%)	Matrix effect[b] mean ± SD (%)
Xanthine	LQC	0.15	0.163 ± 0.006	108.7 ± 4.0	106.8 ± 2.7
	MQC	2.4	2.285 ± 0.031	95.2 ± 1.3	90.9 ± 3.8
	HQC	8	8.289 ± 0.311	103.6 ± 3.9	95.5 ± 3.3
Hypoxanthine	LQC	0.3	0.283 ± 0.009	94.3 ± 3.0	95.8 ± 4.2
	MQC	5	4.863 ± 0.110	97.3 ± 2.2	94.2 ± 4.7
	HQC	8	8.487 ± 0.256	106.1 ± 3.2	103.6 ± 5.1
Guanine	LQC	0.015	0.014 ± 0.001	93.3 ± 6.7	103.7 ± 3.5
	MQC	0.32	0.330 ± 0.013	103.1 ± 4.1	101.7 ± 4.5
	HQC	1.6	1.536 ± 0.072	96.0 ± 4.5	96.6 ± 3.1
Xanthosine	LQC	0.045	0.043 ± 0.002	95.6 ± 4.4	105.6 ± 4.1
	MQC	5	4.661 ± 0.175	93.2 ± 3.5	98.7 ± 2.8
	HQC	12	11.66 ± 0.28	97.2 ± 2.3	96.6 ± 4.6
Inosine	LQC	0.03	0.032 ± 0.001	106.7 ± 3.3	97.4 ± 3.7
	MQC	0.5	0.494 ± 0.019	98.8 ± 3.8	96.0 ± 4.2
	HQC	0.8	0.776 ± 0.045	97.0 ± 5.6	104.5 ± 4.9
Guanosine	LQC	0.009	0.0082 ± 0.0006	91.1 ± 6.7	106.9 ± 3.6
	MQC	0.04	0.041 ± 0.001	102.5 ± 2.5	92.7 ± 3.8
	HQC	0.08	0.079 ± 0.003	98.8 ± 3.8	106.9 ± 4.7
Adenosine	LQC	0.09	0.095 ± 0.003	105.6 ± 3.3	98.5 ± 4.1
	MQC	1.2	1.164 ± 0.041	97.0 ± 3.4	103.4 ± 3.3
	HQC	2.4	2.339 ± 0.088	97.5 ± 3.7	97.1 ± 3.3
Uric acid	LQC	30	28.22 ± 1.45	94.1 ± 4.8	98.5 ± 2.8
	MQC	45	44.14 ± 1.40	98.1 ± 3.1	97.9 ± 3.5
	HQC	90	88.74 ± 2.08	98.6 ± 2.3	102.7 ± 4.8

[a] Recovery (%) = (measured concentration / nominal concentration) × 100 %.
[b] Matrix effect (%) = (peak area in extracted synthetic plasma / peak area in 80 % ACN) × 100 %.

Table 4
Stability (mean ± SD, $n = 6$).

Metabolites	Level	Autosampler (24 h) (RE%)	Freeze-thaw cycles (RE%)
Xanthine	LQC	103.3 ± 3.2	93.3 ± 3.6
	HQC	97.5 ± 3.4	104.8 ± 3.9
Hypoxanthine	LQC	98.4 ± 4.4	97.6 ± 3.9
	HQC	103.6 ± 2.7	98.8 ± 4.7
Guanine	LQC	101.9 ± 3.8	101.6 ± 3.7
	HQC	103.7 ± 2.6	97.7 ± 4.0
Xanthosine	LQC	102.5 ± 3.5	105.1 ± 4.4
	HQC	99.4 ± 3.2	105.8 ± 4.6
Inosine	LQC	96.0 ± 4.6	96.4 ± 3.3
	HQC	96.7 ± 2.9	105.2 ± 4.5
Guanosine	LQC	99.1 ± 3.3	97.3 ± 2.8
	HQC	104.2 ± 4.0	101.9 ± 4.8
Adenosine	LQC	103.5 ± 3.2	103.3 ± 3.1
	HQC	104.4 ± 2.9	98.5 ± 3.3
Uric acid	LQC	96.1 ± 3.6	102.4 ± 4.9
	HQC	96.1 ± 3.5	102.8 ± 3.6

inosine and guanosine were below their LODs. As illustrated in Fig. 3, concentrations of the eight metabolites displayed a wide range of variance, with concentrations ranging from 0.076 to 7.749 μg/mL for xanthine, from 0.179 to 8.251 μg/mL for hypoxanthine, from 0.537 to 12.50 μg/mL for xanthosine, from 0.035 to 2.721 μg/mL for adenosine, from 0.008 to 1.523 μg/mL for guanine, from <LLOQ to 0.095 μg/mL for guanosine, from <LLOQ to 0.929 μg/mL for inosine, and from 18.39 to 94.21 μg/mL for uric acid. Among all the metabolites, uric acid was found to have the highest concentration, followed by xanthine and xanthosine. Adenosine, hypoxanthine, inosine, and guanine were found in small amounts, with guanosine having the lowest concentration. The study concluded that the xanthosine–hypoxanthine–xanthine pathway was responsible for producing uric acid, as depicted in Fig. 1.

3.4. Comparison analysis of purine metabolite with risk factors

In this study, various factors such as age, sex, BMI, smoking, drinking, diet, and bedtime were analyzed to assess the potential risk factors associated with purine metabolism. As demonstrated in Fig. 3B, F and H, no statistically significant associations were found between the concentrations of xanthine, hypoxanthine, guanine, xanthosine, inosine, guanosine, adenosine and uric acid in human plasma with sex, smoking and bedtime ($p > 0.05$). Besides, many participants assessed in the present study had higher plasma uric acid levels related to greater BMI ($p < 0.05$, Fig. 3D) and rich-purine diet ($p < 0.05$, Fig. 3E). Significant associations were also found between xanthine concentrations with BMI, and between xanthine, xanthosine and adenosine concentrations with diet ($p < 0.05$). It was further observed that several purine metabolites such as xanthine, guanine, guanosine and adenosine altered with age and drinking, although there were no statistically significant differences in uric acid concentrations observed (Fig. 3C and F). The results suggested that BMI and diet were the key risk factors associated with purine metabolism disorder, while age and drinking might also play a role.

3.5. ROC analysis of uric acid

The ROC analysis of uric acid levels in the plasma is illustrated in Fig. 4. Our study identified diet and BMI as two of the most significant risk factors, with an area under curve (AUC) of 0.673 and 0.670, respectively. This indicates that individuals with poor dietary habits or higher BMI are at a significantly higher risk of developing abnormal uric acid concentrations in their plasma. Moreover, we found that drinking, smoking, and sex were also strong risk factors, with an AUC ranging from 0.548 to 0.565. On the other hand, age and bedtime were not found to be risk factors, with an AUC of less than 0.5. Our study identified the factors that influenced the levels of uric acid in the plasma, ranked in order of importance as BMI, diet, drinking, sex, smoking, bedtime and age.

4. Conclusions

We developed a novel and rapid HILIC UHPLC-HRMS method for simultaneous and accurate quantification of eight purine metabolites (xanthine, hypoxanthine, guanine, xanthosine, inosine, guanosine, adenosine, and uric acid) in human plasma samples. The method was fully validated, which provided good linearity (R^2 in the range of 0.9931–0.9993), precision (intra- and inter-day RSD in the range of 1.0–6.7 % and 1.3–8.9 %), accuracy (intra- and inter-day RE in the

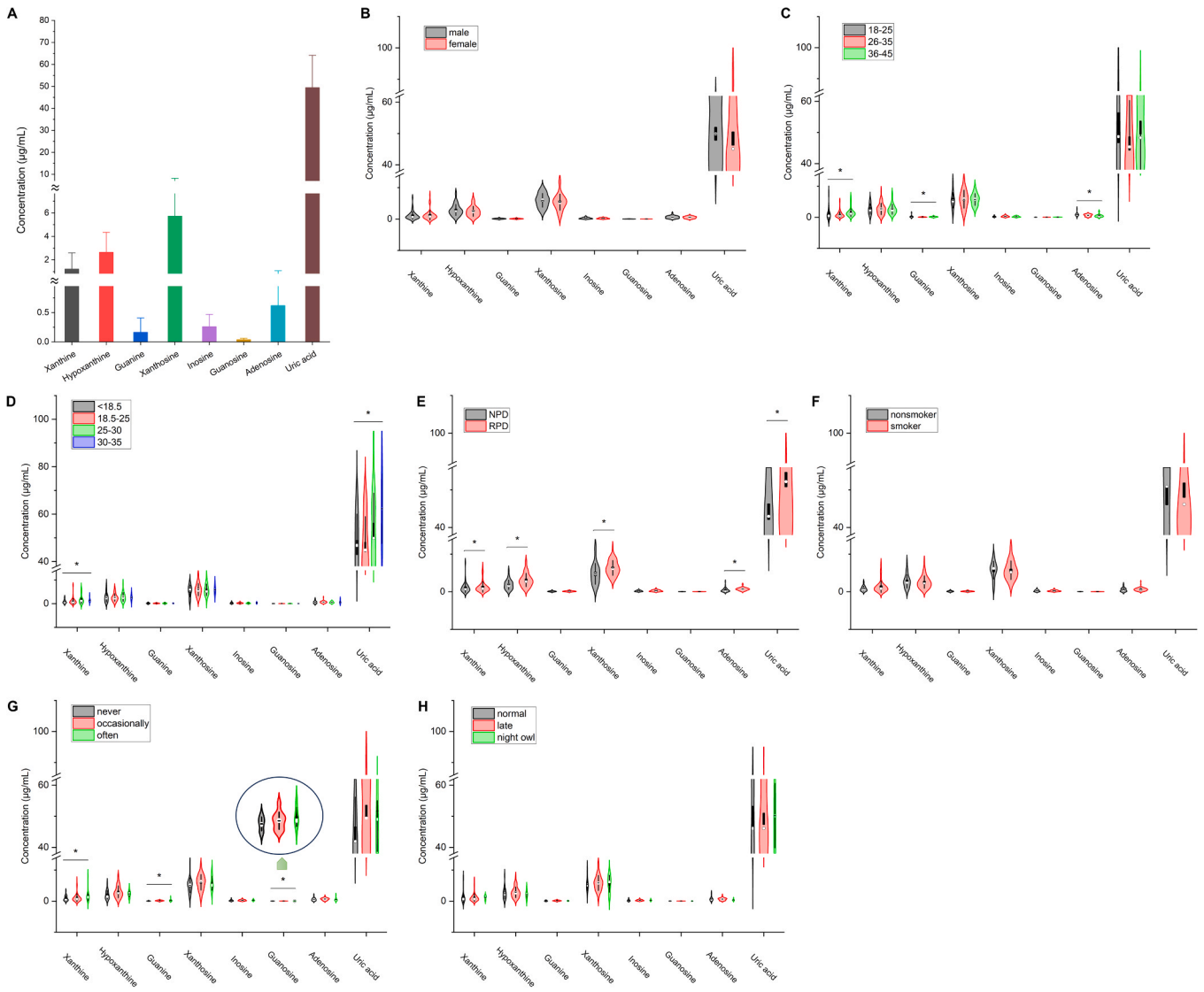

Fig. 3. Concentrations of purine metabolites in plasma. (A) Total concentrations of eight metabolites in plasma samples from 100 healthy participants. (B) Distribution of the metabolites detected in plasma samples from males and females. (C) Distribution of the metabolites detected in plasma samples across different age ranges. (D) Distribution of the metabolites detected in plasma samples from different BMI groups. (E) Distribution of the metabolites detected in plasma samples from participants on normal-purine diet (NPD) and rich-purine diet (RPD) participants. (F) Distribution of the metabolites detected in plasma samples from smoking and non-smoking participants. (G) Distribution of the metabolites detected in plasma samples from different drinking groups. (H) Distribution of the metabolites detected in plasma samples from different bedtime groups. Data are indicated as mean ± standard deviation (SD), * $p < 0.05$, ** $p < 0.01$, *** $p < 0.001$.

range of 92.2–109.5 % and 90.0–110.0 %), and consistency (extraction recovery between 91.1 % and 108.7 %, matrix effect between 90.9 % and 106.9 %, and stability in the range of 93.3–105.8 %). Furthermore, the developed method was successfully applied to monitor the purine metabolism in plasma samples from 100 healthy individuals. The concentrations of different purine metabolites varied dramatically, and the xanthosine–hypoxanthine–xanthine pathway was responsible for producing uric acid. Among the factors, BMI and diet were the key risk factors associated with purine metabolism disorder, age and drinking might also play a role, while sex, smoking and bedtime were not found to be risk factors. In summary, the study provides valuable insights into the potential risk factors for purine metabolite and can be useful in developing preventive and therapeutic strategies for purine metabolism disorders although further studies are needed to understand the exact nature of their association.

Funding

This work was supported by the Scientific Research Project of the Department of Science and Technology of Liaoning Province [grant number 2022-MS-407]; the National Natural Science Foundation of China [grant number 81903793]; the Science and Technology Innovation Fund for graduate students at Shenyang Medical College [grant number Y20220516]; and the Scientific Research Projects for college students at Shenyang Medical College [grant number 20239045].

CRediT authorship contribution statement

Yanming Fang: Resources. **Yingnan Qu:** Formal analysis. **Chuanlong Wu:** Formal analysis. **Qingke Wu:** Data curation. **Rui Liu:** Methodology. **Wenjing Song:** Writing – original draft, Supervision, Conceptualization. **Ronghua Fan:** Writing – review & editing, Funding acquisition. **Jiyangzong De:** Validation.

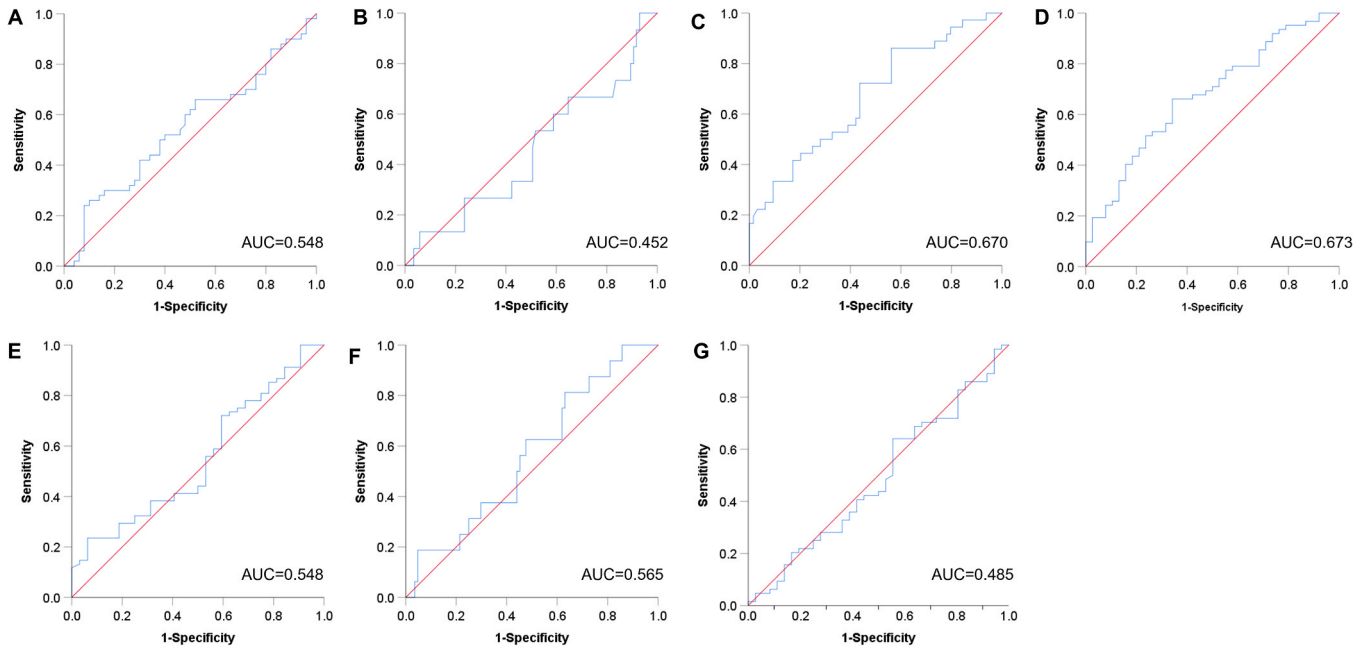

Fig. 4. ROC analysis of the human uric acid in plasma samples versus risk factors. (A) ROC curve of sex factor. (B) ROC curve of age factor. (C) ROC curve of BMI factor. (D) ROC curve of diet factor. (E) ROC curve of smoking factor. (F) ROC curve of drinking factor. (G) ROC curve of sleeping factor.

Declaration of Competing Interest

The authors declare the following financial interests/personal relationships which may be considered as potential competing interests: Ronghua Fan reports financial support was provided by Scientific Research Project of the Department of Science and Technology of Liaoning Province. Ronghua Fan reports financial support was provided by National Natural Science Foundation of China. If there are other authors, they declare that they have no known competing financial interests or personal relationships that could have appeared to influence the work reported in this paper.

Acknowledgements

Thank Dr. Lizhen Qiao for providing the HILIC column required for this work.

Appendix A. Supporting information

Supplementary data associated with this article can be found in the online version at doi:10.1016/j.jpba.2024.116451.

References

[1] J.E. Seegmiller, Purine metabolism, Arthritis Rheum. 18 (1975) 681–686.
[2] K.L. Nelson, V.S. Voruganti, Purine metabolites and complex diseases: role of genes and nutrients, Curr. Opin. Clin. Nutr. Metab. Care 24 (2021) 296–302.
[3] N. Zollner, Purine and pyrimidine metabolism, P. Nutr. Soc. 41 (1982) 329–342.
[4] J.H. Topps, R.C. Elliott, Relationship between concentrations of ruminal nucleic acids and excretion of purine derivatives by sheep, Nature 205 (1965) 498–499.
[5] C. Scazzocchio, The purine degradation pathway, genetics, biochemistry and regulation, Prog. Ind. Microbiol. 29 (1994) 221–257.
[6] J.B. Wyngaarden, Overproduction of uric acid as the cause of hyperuricemia in primary gout, J. Clin. Invest. 36 (1957) 1508–1515.
[7] S.F. Keller, B.F. Mandell, Management and cure of gouty arthritis, Rheum. Dis. Clin. North. Am. 48 (2022) 479–492.
[8] S.Y. Su, T.H. Lin, Y.H. Liu, P.Y. Wu, J.C. Huang, H.M. Su, S.C. Chen, Sex difference in the associations among obesity-related indices with hyperuricemia in a large Taiwanese population study, Nutrients 15 (2023) 3419.
[9] C.F. Xu, Hyperuricemia and nonalcoholic fatty liver disease: from bedside to bench and back, Hepatol. Int. 10 (2016) 286–293.
[10] T. Dogru, H. Genc, S. Tapan, S. Bagci, Hyperuricemia in non-alcoholic fatty liver disease, Aliment. Pharm. Ther. 34 (2011) 1042–1043.
[11] I. Mortada, Hyperuricemia, type 2 diabetes mellitus, and hypertension: an emerging association, Curr. Hypertens. Rep. 19 (2017) 69.
[12] S. Zhang, Y. Wang, J. Cheng, N. Huangfu, R. Zhao, Z. Xu, F. Zhang, W. Zheng, D. Zhang, Hyperuricemia and cardiovascular disease, Curr. Pharm. Des. 25 (2019) 700–709.
[13] Y. Saito, A. Tanaka, K. Node, Y. Kobayashi, Uric acid and cardiovascular disease: a clinical review, J. Cardiol. 78 (2021) 51–57.
[14] D.M. Williams, S. Hägg, N.L. Pedersen, Circulating antioxidants and Alzheimer disease prevention: a Mendelian randomization study, Am. J. Clin. Nutr. 109 (2019) 90–98.
[15] R. Bakshi, E.A. Macklin, R. Logan, M.M. Zorlu, N. Xia, G.F. Crotty, E. Zhang, X. Chen, A. Ascherio, M.A. Schwarzschild, Higher urate in LRRK2 mutation carriers resistant to Parkinson disease, Ann. Neurol. 85 (2019) 593–599.
[16] S. Mi, L. Gong, Z. Sui, Friend or foe? An unrecognized role of uric acid in cancer development and the potential anticancer effects of uric acid-lowering drugs, J. Cancer 11 (2020) 5236–5244.
[17] A. Tiku, D.W. Johnson, S.V. Badve, Recent evidence on the effect of urate-lowering treatment on the progression of kidney disease, Curr. Opin. Nephrol. Hy. 30 (2021) 346–352.
[18] R. Floege, R.J. Johnson, Hyperuricemia and progression of chronic kidney disease: to treat or not to treat? Kidney Int 99 (2021) 14–16.
[19] Y. Wang, M. Deng, B. Deng, L. Ye, X. Fei, Z. Huang, Study on the diagnosis of gout with xanthine and hypoxanthine, J. Clin. Lab Anal. 33 (2019) e22868.
[20] N. Cooper, R. Khosravan, C. Erdmann, J. Fiene, J.W. Lee, Quantification of uric acid, xanthine and hypoxanthine in human serum by HPLC for pharmacodynamic studies, J. Chromatogr. B. 837 (2006) 1–10.
[21] A. Andries, S. De Rechter, P. Janssens, D. Mekahli, A. Van Schepdael, Simultaneous determination of allantoin and adenosine in human urine using liquid chromatography-UV detection, J. Chromatogr. B. 1096 (2018) 201–207.
[22] E. Caussé, A. Pradelles, B. Dirat, A. Negre-Salvayre, R. Salvayre, F. Couderc, Simultaneous determination of allantoin, hypoxanthine, xanthine, and uric acid in serum/plasma by CE, Electrophoresis 28 (2007) 381–387.
[23] Z.B. Chen, C.H. Huang, W. Liu, L. Zhang, P. Tong, L. Zhang, Simultaneous determination of nucleoside and purine compounds in human urine based on a hydrophobic monolithic column using capillary electrochromatography, Electrophoresis 36 (2015) 2727–2735.
[24] C.X. Liu, C.Y. Gu, W. Huang, X. Sheng, J. Du, Y.B. Li, Targeted UPLC-MS/MS high-throughput metabolomics approach to assess the purine and pyrimidine metabolism, J. Chromatogra. B. 1113 (2019) 98–106.
[25] A. Cremonesi, D. Meili, A. Rassi, M. Poms, B. Tavazzi, V. Škopová, J. Häberle, M. Zikánová, M. Hersberger, Improved diagnostics of purine and pyrimidine metabolism disorders using LC-MS/MS and its clinical application, Clin. Chem. Lab Med. 61 (2023) 1792–1801.
[26] B. Tavazzi, G. Lazzarino, P. Leone, A.M. Amorini, F. Bellia, C.G. Janson, V. Di Pietro, L. Ceccarelli, S. Donzelli, J.S. Francis, B. Giardina, Simultaneous high performance liquid chromatographic separation of purines, pyrimidines, N-acetylated amino acids, and dicarboxylic acids for the chemical diagnosis of inborn errors of metabolism, Clin. Biochem. 38 (2005) 997–1008.
[27] G. Zhang, A.D. Walker, Z. Lin, X. Han, M. Blatnik, R.C. Steenwyk, E.A. Groeber, Strategies for quantitation of endogenous adenine nucleotides in human plasma

using novel ion-pair hydrophilic interaction chromatography coupled with tandem mass spectrometry, J. Chromatogr. A. 1325 (2014) 129–136.
[28] N. Marklund, B. Ostman, L. Nalmo, L. Persson, L. Hillered, Hypoxanthine, uric acid and allantoin as indicators of in vivo free radical reactions. Description of a HPLC method and human brain microdialysis data, Acta Neurochir. (Wien.). 142 (2000) 1135–1141.
[29] X. Li, Z. Liu, Z. Li, X. Xiong, X. Zhang, C. Yang, L. Zhao, R. Zhao, A simple, rapid and sensitive HILIC LC-MS/MS method for simultaneous determination of 16 purine metabolites in plasma and urine, Talanta 267 (2024) 125171.
[30] T. Ikegami, K. Tomomatsu, H. Takubo, K. Horie, N. Tanaka, Separation efficiencies in hydrophilic interaction chromatography, J. Chromatogr. A. 1184 (2008) 474–503.
[31] Z. Lu, S. Li, N. Aa, Y. Zhang, R. Zhang, C. Xu, S. Zhang, X. Kong, G. Wang, J. Aa, Y. Zhang, Quantitative analysis of 20 purine and pyrimidine metabolites by HILIC-MS/MS in the serum and hippocampus of depressed mice, J. Pharm. Biomed. Anal. 219 (2022) 114886.
[32] A. Andries, A. Feyaerts, D. Mekahli, A. Van Schepdael, Quantification of allantoin and other metabolites of the purine degradation pathway in human plasma samples using a newly developed HILIC-LC-MS/MS method, Electrophoresis 43 (2022) 1010–1018.
[33] B. Rochat, From targeted quantification to untargeted metabolomics: why LC-high-resolution-MS will become a key instrument in clinical labs, Trends Anal. Chem. 81 (2016) 151–164.
[34] M. Stommel, C.A. Schoenborn, Accuracy and usefulness of BMI measures based on self-reported weight and height: findings from the NHANES & NHIS 2001-2006, BMC Public Health 9 (2009) 421.
[35] L. Qiao, W. Lv, M. Chang, X. Shi, G. Xu, Surface-bonded amide-functionalized imidazolium ionic liquid as stationary phase for hydrophilic interaction liquid chromatography, J. Chromatogr. A. 1559 (2018) 141–148.